PAPER • OPEN ACCESS

A robust plasma-based laser amplifier via stimulated Brillouin scattering

View the article online for updates and enhancements.

You may also like

IOP ebooks™

Bringing together innovative digital publishing with leading authors from the global scientific community.

Start exploring the collection–download the first chapter of every title for free.

A robust plasma-based laser amplifier via stimulated Brillouin scattering

E P Alves[1,2,9] , **R M G M Trines**[3,9,*] , **K A Humphrey**[4], **R Bingham**[3,4] , **R A Cairns**[5] , **F Fiúza**[6,8], **R A Fonseca**[1,7] **and L O Silva**[1]

[1] GoLP/Instituto de Plasmas e Fusão Nuclear, Instituto Superior Técnico, Universidade de Lisboa, 1049-001 Lisbon, Portugal

[2] Department of Physics and Astronomy, University of California Los Angeles, Los Angeles, CA 90095, United States of America

[3] Central Laser Facility, STFC Rutherford Appleton Laboratory, Didcot OX11 0QX, United Kingdom

[4] SUPA, Department of Physics, University of Strathclyde, Glasgow G4 0NG, United Kingdom

[5] University of St Andrews, St Andrews, Fife KY16 9SS, United Kingdom

[6] Lawrence Livermore National Laboratory, Livermore, CA, United States of America

[7] DCTI/ISCTE Lisbon University Institute, 1649-026 Lisbon, Portugal

[8] High Energy Density Science Division, SLAC National Accelerator Laboratory, Menlo Park, CA 94025, United States of America

E-mail: raoul.trines@stfc.ac.uk

CrossMark

Abstract

Brillouin amplification in plasma is more resilient to fluctuations in the laser and plasma parameters than Raman amplification, making it an attractive alternative to Raman amplification. In this work, we focus on high plasma densities, $n_0 > n_{cr}/4$, where stimulated Raman scattering is not possible and laser beam filamentation is the dominant competing process. Through analytic theory and multi-dimensional particle-in-cell simulations, we identify a parameter regime for which Brillouin amplification can be efficient while maintaining filamentation of the probe at a controlled level. We demonstrate pump-to-probe compression ratios of up to 72 and peak amplified probe fluences over 1 kJ cm^{-2} with $\simeq 50\%$ efficiency. High pulse quality is maintained through control of parasitic filamentation, enabling operation at large beam diameters. Provided the pump and probe pulse diameters can be increased to 1 mm, our results suggest that Brillouin amplification can be used to produce sub-picosecond pulses of petawatt power.

Keywords: Brillouin amplification, parametric instabilities, laser-plasma interactions, high energy density physics

(Some figures may appear in colour only in the online journal)

---

1. Introduction

Amplification of laser beams via parametric instabilities in plasma (stimulated Raman and Brillouin scattering) has been proposed a number of times [1–5], but came into its own only relatively recently [6–19]. This has been accompanied by an increasing effort to optimize the parameters for the interaction via numerical simulations [20–26]. Further recent work includes the study of Raman amplification of x-rays [27, 28], the use of chirped laser pulses in Brillouin amplification [29, 30] and the study of numerous novel configurations for pulse amplification [31–37]. Brillouin scattering has also been used to transfer energy via the cross-beam energy transfer scheme at the national ignition facility [38–44]. Both Raman and Brillouin scattering have been studied extensively in the context of Inertial Confinement Fusion [45–56]; Raman scattering also in the context of wakefield acceleration [57–66]. Raman and Brillouin scattering are processes where two electromagnetic waves at slightly different frequencies propagating in plasma exchange energy via a plasma wave. For Raman scattering, this is a fast electron plasma wave, while for Brillouin scattering it is a slower ion-acoustic wave [67]. When it comes to laser beam amplification, Raman and Brillouin scattering have different properties and serve different purposes. Raman amplification yields the shortest output pulses and the highest amplification ratios, but it is sensitive to fluctuations in the experimental parameters and requires high accuracy in the matching of laser and plasma frequencies. Brillouin amplification yields lower peak intensities or amplification ratios, but is far more robust to parameter fluctuations or frequency mismatch, more efficient (as less laser energy stays behind in the plasma wave) and more suitable for the production of pulses with a high total power or energy.

For both Raman and Brillouin amplification, two main goals can be identified: first, maximizing the final power and energy content of the pumped pulse, and second, ensuring that the pumped pulse has the best possible quality, i.e. a smooth envelope and a high contrast (low-intensity pre-pulse). Production of kilojoule, picosecond laser pulses of good quality using Raman amplification has been explored by Trines *et al* [14, 16]. Here it will be shown that a similar approach also works for Brillouin amplification in the so-called 'strong coupling' regime [10].

Strongly coupled Brillouin amplification can be carried out in basically two plasma density regimes: $n_0/n_{cr} > 0.25$ and $n_0/n_{cr} < 0.25$. Here, n_0 denotes the plasma electron density and n_{cr} denotes the 'critical' density above which the pump beam can no longer propagate. These regimes are distinguished by different trade-offs in the control of parasitic instabilities that can develop during the Brillouin amplification process. For $n_0/n_{cr} < 0.25$, one sees lower growth of various instabilities like filamentation [68], while for $n_0/n_{cr} > 0.25$ stimulated Raman scattering (SRS) is forbidden [67], eliminating a significant class of damaging instabilities. Also, the growth rate for Brillouin scattering is higher for higher plasma densities [67], leading to faster growth of the Brillouin-amplified pulse and a higher compression ratio [26]. Recent experimental and numerical studies have focused

on $n_0/n_{cr} < 0.25$ densities (specifically in the range $0.05 \leq n_0/n_{cr} \leq 0.15$) [13, 18, 19, 21, 23, 70, 71]. These works thus accept the presence of parasitic SRS in exchange for a lower growth of the filamentation instability. The original work by Andreev *et al* [10] demonstrated efficient strongly coupled Brillouin amplification at $n_0/n_{cr} = 0.3$ (where all SRS is forbidden) using one-dimensional particle-in-cell (PIC) simulations. These, however, did not capture the interplay with the ponderomotive filamentation instability (which develops transverse to the propagation direction), which is the most dangerous instability at such high densities.

In this work, we revisit sc-Brillouin amplification at densities $n_0/n_{cr} > 0.25$, and we investigate its self-consistent interplay with filamentation by means of large-scale two-dimensional (2D) PIC simulations. We give a brief summary of the self-similar theory from our earlier work [26], as we use the self-similar scalings to design our numerical simulations. We further derive new scalings for sc-Brillouin amplification performance that take into account the limiting effects of probe filamentation. These scalings describe how sc-Brillouin amplification and compression vary with pump intensity for a fixed tolerance level of probe filamentation; we show that filamentation can be offset by operating at lower pump intensities, improving overall sc-Brillouin amplification performance. Finally, we present 2D PIC simulations that self-consistently capture the interplay between sc-Brillouin amplification and filamentation, which support our theoretical scalings.

2. Scaling laws in the self-similar regime

In this paper, we will exploit recent results on the properties of Brillouin-amplified pulses in the nonlinear pump-depletion regime [26]. In the pump-depletion regime, the growing seed pulse is 'self-similar', meaning that an advance in time corresponds to a rescaling of the pulse's duration and amplitude, without changing the basic shape of the pulse. This leads to stronger amplification at higher efficiencies, as explained in detail in [26], and also seen in a recent experiment [19].

In [26], it was shown that the seed pulse amplitude a_{pr} and duration τ_{pr} are no longer independent in the pump-depletion regime, but evolve together according to well-defined scaling laws (equations (1) and (2) below). We can exploit these laws in two ways. Before the interaction, we can tailor the seed pulse to launch the interaction directly into the efficient pump-depletion regime, skipping the inefficient 'linear' regime of amplification altogether. After the interaction, we can use these laws to predict the properties of the amplified seed pulse, and also to determine how 'non-linear' the seed pulse has become, as a measure of the quality of our amplification (see figure 1 and accompanying discussion below).

To explore how the intensity and duration of a Brillouin-amplified probe pulse can be controlled, we use the self-similar model of Andreev *et al* [10] for Brillouin amplification in the strong-coupling regime (high pump intensity). We start from a homogeneous plasma with electron number density n_0, plasma frequency $\omega_p^2 = e^2 n_0/(\varepsilon_0 \, m_e)$ [ion
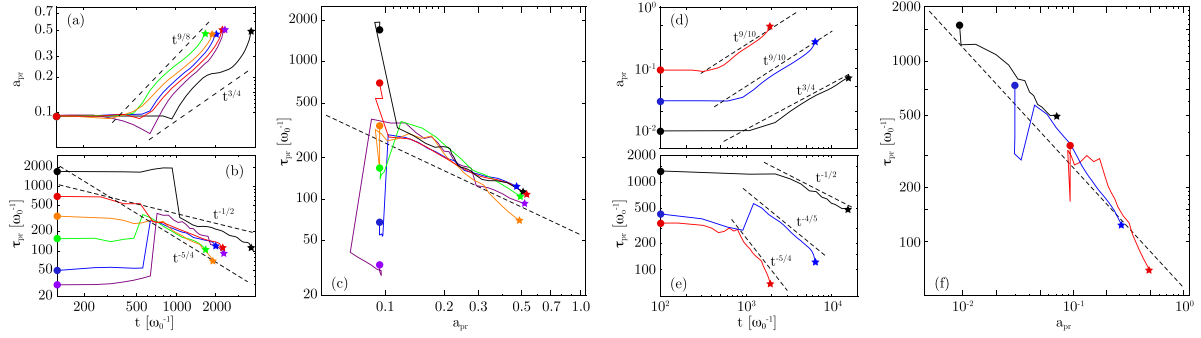
Figure 1. Verification of the scaling laws for the amplitude, duration, and triple product $a_{pr}^{2/3}\Gamma_{sc}$ for a Brillouin-amplified pulse. (a)–(c): temporal evolution of (a) probe amplitude a_{pr} and (b) probe duration τ_{pr} for different initial probe durations, $\tau_{pr}/\tau_{opt} = 0.1$ (purple curve), $\tau_{pr}/\tau_{opt} = 0.2$ (blue curve), $\tau_{pr}/\tau_{opt} = 0.5$ (green curve), $\tau_{pr}/\tau_{opt} = 1$ (orange curve), $\tau_{pr}/\tau_{opt} = 2$ (red curve), and $\tau_{pr}/\tau_{opt} = 5$ (black curve); the initial probe and pump intensity are fixed at 10^{16} W cm^2, assuming 1 μm laser light; the plasma density is $n_0/n_{cr} = 0.3$. The paths traced by the amplifying probe pulses in the (a_{pr}, τ_{pr}) phase space is shown in (c); the dashed line represents equation (2). (d)–(f): temporal evolution of (d) probe amplitude a_{pr} and (e) probe duration τ_{pr} for different pump intensities, 10^{14} W cm^{-2} (black curve), 10^{15} W cm^{-2} (blue curve) and 10^{16} W cm^{-2} (red curve), assuming 1 μm laser light; the plasma density is $n_0/n_{cr} = 0.3$. The initial amplitude of the probe is the same as the pump amplitude, for each case, and the initial probe duration is chosen according to τ_{opt}. The circle and star markers represent the initial and final states of the amplification process, respectively. The paths traced by the probe pulses in the (a_{pr}, τ_{pr}) phase space is shown in (f); the dashed line represents equation (2). Note that all axes in ((a)–(f)) are presented in logarithmic scale.

plasma frequency $\omega_{pi} = \omega_p \sqrt{Zm_e/m_i}$], electron/ion temperatures T_e and T_i, and a pump laser pulse with wave length λ, intensity I, frequency $\omega_0 = 2\pi c/\lambda$, dimensionless amplitude $a_{pu} \equiv 8.55 \times 10^{-10} \sqrt{g} \sqrt{I\lambda^2[\mathrm{Wcm^{-2}\mu m^2}]}$, where $g = 1$ ($g = 1/2$) denotes linear (circular) polarization, and wave group speed $v_g/c = \sqrt{1 - \omega_p^2/\omega_0^2} = \sqrt{1 - n_0/n_{cr}}$. Let the durations of pump and probe pulse be given by τ_{pu} and τ_{pr}, and define Γ_{sc} as $\Gamma_{sc}^3 = (v_g/c)^2 \omega_{pi}^2 \omega_0/(2g) = \omega_0^3(Zm_e/m_i)(n_0/n_{cr})(1 - n_0/n_{cr})/(2g)$, the coupling constant for Brillouin scattering in the strong-coupling regime [26, 67]. Following our earlier results, we obtain the following relations between pulse amplitudes and durations [26]:

$$\Gamma_{sc}^3 a_{pu}^2 \, \tau_{pu}\tau_{pr}^2 \approx 22, \qquad (1)$$

$$\Gamma_{sc} a_{pr}^{2/3}\tau_{pr} \approx (13.8)^{1/3} \approx 2.40. \qquad (2)$$

This means that the initial probe pulse duration is not a free parameter: equation (2) dictates the optimal initial probe pulse duration τ_{opt} for a given initial probe pulse amplitude a_{pr}. From previous numerical work on Raman [16, 69] and Brillouin amplification [20, 21], it follows that if the probe pulse is too short for its amplitude initially, it will first generate a much longer secondary probe pulse behind the original probe [which does fulfill equation (2)] and this secondary probe will then amplify while the original short probe will hardly gain in intensity. Thus, trying to produce ultra-short laser pulses via Brillouin amplification by reducing the initial pulse duration simply does not work. Earlier attempts in this direction [70, 71] showed no increase in total pulse power (as opposed to pulse peak intensity), confirming the results of [20, 21]. An in-depth discussion of these matters can be found in [26].

From the model by Andreev *et al* [10], the seed pulse amplitude and duration are predicted to scale ideally as $a_{pr}(t) \propto$ $(a_{pu}^2 \, \Gamma_{sc}t)^{3/4}$ and $\tau_{pr}(t) \propto (a_{pu}^2 \, \Gamma_{sc}t)^{-1/2}$. From our own work [26], we find that $a_{pr}^{2/3}(t)\Gamma_{sc}\tau_{pr}(t)$ ideally remains constant in time, see equation (2) above. We have tested these scaling laws in 1D PIC simulations of Brillouin amplification where we varied the initial seed duration between $0.1 < \tau_{pr}/\tau_{opt} < 5$ and the pump intensity between $10^{14} < I_{pu} < 10^{16}$ W cm^{-2}; we considered a plasma density of $n_0/n_{cr} = 0.3$ and the initial probe intensity was matched to the pump. The results are displayed in figure 1. Within this range of parameters, we find that the seed pulse amplitude scales as $a_{pr}(t) \propto (a_{pu}^2 \, \Gamma_{sc}t)^{\alpha}$ with $0.75 \leq \alpha \leq 0.9$, while $\tau_{pr}(t) \propto (a_{pu}^2 \, \Gamma_{sc}t)^{-\beta}$ with $0.5 \leq \beta \leq 1.25$. The triple product $a_{pr}^{2/3}(t)\Gamma_{sc}\tau_{pr}(t)$ remains nearly constant though, once it has settled on its optimal value, so its scaling proves more robust than that of $a_{pr}(t)$ or $\tau_{pr}(t)$ individually.

For high plasma densities, where Raman scattering is not possible, further scaling laws can be found in addition to the above ones for a_{pr} and τ_{pr}. For the filamentation of the probe pulse, we have $\gamma_f \propto a_{pr}^2$, so $\int \gamma_f dt \propto a_{pu}^3 t^{5/2}$. We can keep the level of filamentation, and thus $\int \gamma_f dt$ constant by choosing $\tau_{pu} \propto I_{pu}^{-3/5}$, where I_{pu} denotes the pump intensity. This leads to $\tau_{pr}(t) \propto I_{pu}^{-1/5}$ and $I_{pr} \propto a_{pr}^2(t) \propto I_{pu}^{3/5}$. Thus, the compression and amplification ratios both scale as $\tau_{pu}/\tau_{pr} \propto I_{pr}/I \propto I_{pu}^{-2/5}$ (under the assumption that the efficiency is mostly constant). Finally, we find that the pump pulse energy fluence scales as $F \propto I_{pu}\tau_{pu} \propto I_{pu}^{2/5}$. All these scalings are subject to the assumption that one is operating in the 'self-similar' (non-linear, pump-depletion) phase of the strong-coupling regime for Brillouin scattering, $a_{pu}^2 > 4(v_T/c)^3(n_{cr}/n_0)\sqrt{1 - n_0/n_{cr}}\sqrt{Zm_e/m_i}$ or $I_{pu} > 1.6 \times 10^{13}$ W cm^{-2} for our parameters. Already it was found that for $I_{pu} = 10^{14}$ W cm^{-2}, the growing probe did not fully conform to the above scaling laws because I_{pu} is too close to the strong-coupling threshold. Lowering the ion temperature from
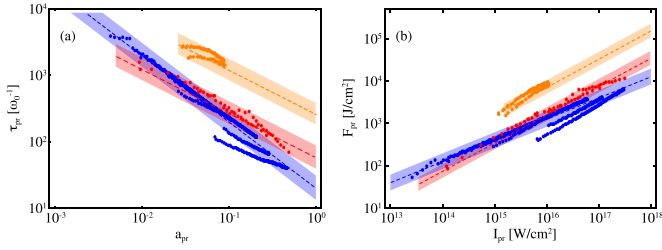
Figure 2. (a) Map of (a_{pr}, τ_{pr}) of successfully amplified seed pulses via Raman amplification (blue), sc-Brillouin amplification at over-quarter-critical densities (red) and sc-Brillouin amplification at sub-quarter-critical densities (orange). The points are taken from 1D PIC simulations while the shaded areas indicate predictions by equation (2) or (3). The simulation points correspond to the entire evolution of the amplified seed from multiple simulations using different parameters of plasma density and pump intensity. (b) The same data shown on the left is presented in a map of seed fluence versus seed intensity, for 1 μm pump pulse wave length.

500 to 50 eV appears to lower the strong-coupling threshold also, bringing the behavior of the $I_{pu} = 10^{14}$ W cm^{-2} case closer to pure strong-coupling Brillouin amplification and improving its amplification and compression ratios. While ion wave breaking has been observed in one-dimensional simulations [10], with a characteristic time of $\tau_{wb} \propto I_{pu}^{-1/2}$ [67, 81], it did not play a major role in the two-dimensional simulations presented above, since filamentation always emerged earlier for pump intensities in the strong-coupling regime. From this, it is clear that, when the pump intensity is decreased, Brillouin amplification improves on all fronts.

Knowledge of the scaling laws for Brillouin and Raman amplification [6, 10, 26] allows one to compare these two mechanisms for pulse compression in plasma, and to determine which mechanism is most suitable to obtain an output pulse with specific properties. We recall that the Raman equivalent of equation (2) is given by [26]:

$$||a_{pr}||\Gamma_R\tau_{pr} \approx 3.4, \tag{3}$$

with $\Gamma_R = [\omega_0 \omega_{pe}/(4g)]^{1/2} = \omega_0(n_e/n_{cr})^{1/4}/\sqrt{4g}$. In figure 2, we compare successful 1D simulations of Raman amplification at $0.0025 < n_0/n_{cr} < 0.01$ (blue) and sc-Brillouin amplification at $m_i/(Zm_e) = 1836$, $0.275 < n_0/n_{cr} = 0.325$ (red) and $0.0075 < n_0/n_{cr} = 0.0125$ (orange). The density ranges have been chosen to minimize the impact of unwanted instabilities [14]. The dots mark the simulation results, while the shaded areas mark the predictions by equations (2) or (3). Frame (a) shows the duration τ_{pr} versus the amplitude a_{pr} for the amplified seed, while frame (b) shows the energy flux $F_{pr} = I_{pr}\tau_{pr}$ versus intensity I_{pr} for the same cases. All simulation points lie within the theoretically predicted shaded regions that correspond to the attractor solution, highlighting the robustness of scaling laws like (2) and (3) for a very broad range of parameters. As intuitively expected, Raman amplification is capable of producing the shortest pulses and highest intensities, although pulses produced by strongly coupled Brillouin amplification at over-quarter-critical densities are very similar in these respects. Brillouin

amplification at lower plasma densities reaches lower peak intensities but yields the highest pulse fluence because of longer pulse durations. These results serve as an important guide when choosing not only the laser and plasma parameters, but also the amplification scheme (Raman for short pulses with high intensity, Brilouin for the highest energy transfer) when designing an experiment to obtain a desired output pulse.

3. Simulations

To further investigate Brillouin amplification, in particular limiting factors such as filamentation and wave breaking of the ion wave, we have carried out a sequence of PIC simulations using OSIRIS [72–74]. Parameters varied in these simulations are the pump intensity ($I_{pu} = 10^{14}$, 10^{15} and 10^{16} W cm^{-2}) and the interaction length. The laser wave length was $\lambda = 1$ μm and the plasma density was set at $n_0/n_{cr} = 0.3$, to eliminate parasitic Raman scattering. Such scattering can do great damage to the envelope of the amplified pulse, as discussed below. The ion-electron mass ratio was $m_p/m_e = 1836$ and $T_e = T_i = 500$ eV. For our choices of plasma density and temperature and pump laser intensities, the electron-ion collision frequency ν_{ei} is always significantly lower than the sc-Brillouin growth rate $\Gamma_{sc}a_{pu}^{2/3}$, which is itself lower again than the inverse pump depletion time $\Gamma_{sc}a_{pr}^{2/3}$. Hence collisional effects are not expected to impact the amplification process. All our simulations use pump intensities above the strong-coupling threshold, which corresponds to 3.8×10^{13} W cm^{-2} for the plasma conditions considered. The initial probe pulse intensity was chosen to be the same as the pump intensity, and the initial probe duration was half the value predicted by (2), because this yielded a somewhat better performance, see [26] for details. The plasma column was given a constant density, while the plasma length was determined dynamically as these simulations were conducted in a moving window that follows the seed pulse (at v_g), with the pump pulse implemented as a boundary condition at the leading edge [75, 76]. We note that we use the moving window technique for computational efficiency in modeling the self-consistent multi-dimensional dynamics of the seed pulse, but it does not capture the full propagation of the pump in the plasma column, and hence does not capture thermal scatter and other pump instabilities that may arise before meeting the seed. The moving window is thus only a valid approximation when such pump instabilities can be controlled before meeting the probe. Indeed, recently proposed 'flying focus' techniques [82] provide a viable approach to controlling premature pump instabilities, allowing to closely approximate the conditions of our moving window simulations.

We have performed two-dimensional moving window simulations, using a spatial resolution of $dx = \lambda_D/2$ and $dy = 0.5c/\omega_0$, with 25 particles per cell per species and quadratic interpolation for the current deposition. Both pump and probe pulses have identical transverse Gaussian envelopes, with waist sizes (W_0) of $W_0 = 1000c/\omega_0 = 160$ μm for the 10^{15} and 10^{16} W cm^{-2} scenarios, and $W_0 = 1500c/\omega_0 = 240$ μm for the 10^{14} W cm^{-2} scenario; these focal spots are chosen
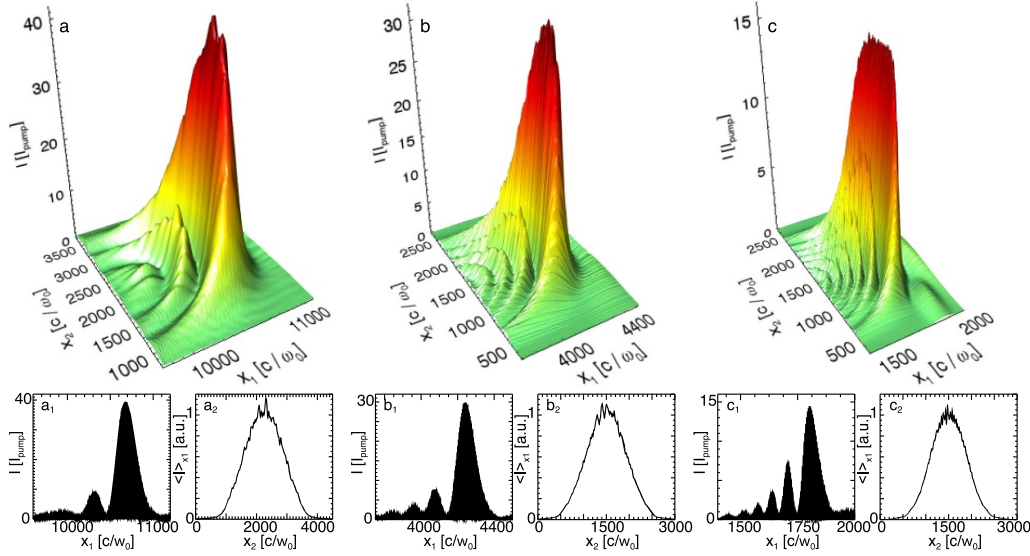
Figure 3. Brillouin-amplified probe pulses for pump/probe intensities of (a) 10^{14}, (b) 10^{15} and (c) 10^{16} W cm^{-2} for $n_0/n_{cr} = 0.3$. Pump pulse durations are 11.4, 3.8 and 1.1 ps respectively. The 3D visualizations illustrate the amplified probe pulses at 10% filamentation level. Frames a_1–c_1 show the longitudinal intensity profile taken at the center of the probe, and frames a_2–c_2 show the average transverse intensity profile along the longitudinal direction normalized to the average peak intensity.

to be wide enough to contain >6 filamentation wavelengths at their respective initial intensity. The probe pulses have $\sin^2$ temporal profiles, with durations corresponding to $\tau_{pr} = \tau_{opt}/2$ determined from (2). The pump pulses have a flat temporal profile with a short rise time of $500 \, \omega_0^{-1} \simeq 260$ fs.

For $n_0/n_{cr} = 0.3$ there will be no Raman backscattering from noise by the pump, i.e. no significant prepulse, and no modulation of the probe pulse envelope by Raman forward scattering. Thus, transverse filamentation of the probe pulse becomes the limiting factor for amplification, while self-focusing [77–79] and wave breaking are found to be insignificant. The evolution of each 2D simulation was followed until transverse fluctuations of the probe envelope induced by filamentation reached 10% of the probe peak intensity. At this point, the pump-probe interaction was considered to terminate, setting the pump pulse duration and plasma column length. Using this criterion, pump pulse durations of 11.4, 3.8 and 1.1 ps were obtained for $I_{pu} = 10^{14}$, 10^{15} or 10^{16} W cm^{-2} respectively. Results are shown in figure 3. The top row shows the 2D intensity envelopes of the amplified pulses, while the bottom row shows longitudinal and transverse intensity profiles. The 2D plots reveal that there is no reduction of the probe pulse diameter, allowing amplification to high total powers, not just high intensities. The intensity envelopes are smooth, with filamentation fluctuations not exceeding 10%. This is in contrast to the results of references [70, 71], which are strongly modulated by filamentation and Raman forward scattering and exhibit a fourfold reduction in spot diameter. Filamentation usually occurs when either the pulse intensities are too high or the interaction length is too long; a typical example of out-of-control filamentation, for a pump pulse at 10^{16} W cm^{-2} and 2 ps duration, is shown in figure 4(a).

4. Discussion

We define the *compression ratio* as the duration of the pump pulse divided by the duration of the amplified probe, and the *amplification ratio* as the intensity of the amplified probe divided by the intensity of the pump. We then find compression ratios of 40, 60 and 72, and amplification ratios of 15, 30 and 40, for pump intensities of 10^{16}, 10^{15} and 10^{14} W cm^{-2} respectively. The increase in these ratios with decreasing pump intensity follows from the fact that the filamentation growth rate decays more rapidly with decreasing pulse intensity than the sc-Brillouin scattering growth rate. Of course, operating at lower pulse intensities requires the use of longer interaction lengths and plasma columns. This could potentially introduce other difficulties such as increased premature Brillouin backscattering of the pump before it meets the probe. However, as mentioned earlier, this may be circumvented by utilizing advanced pump focusing schemes such as the 'flying focus' [82], where one can avoid propagating the intense pump through the entire plasma column before it meets the probe.

We find that the absolute duration of the amplified probe increases with decreasing pulse intensity, as follows from equation (1), emphasizing that Brillouin amplification works best for longer pulses at lower intensities. The main peak of the amplified pulse is followed by a sequence of secondary peaks, as predicted by one-dimensional theory and simulations [10, 20, 21]. The amplified pulses have a 'bowed' shape, as also seen for Raman amplification [14, 16, 80]. This can be understood from the self-similar theory: the pump intensity is highest on-axis and decreases for larger radius, so the probe duration is shortest on-axis and increases for larger radius, leading to the characteristic horseshoe shape. The energy transfer efficiency from the pump to the main peak of
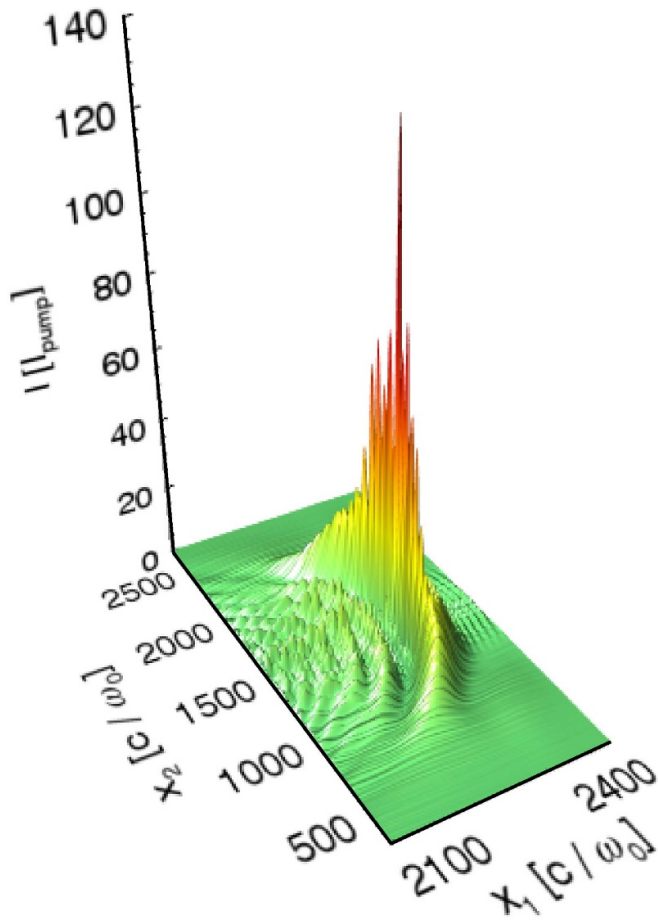
Figure 4. Parasitic filamentation associated with Brillouin amplification in over-quarter-critical plasma ($n_0/n_{cr} = 0.3$). Pulse intensities are 10^{16} W cm^{-2}. The probe's transverse intensity profile is distorted due to filamentation.

the amplified probe is found to be approximately 50% for each case.

We note that in our simulations we have considered ideal pump and probe beams with initially smooth envelopes and phase fronts. However, realistic laser beams in experiments may contain aberrations in both the phase front and envelope (so-called speckles), which can degrade Brillouin amplification performance and need to be taken into account. When a speckled pump beam interacts with the plasma column prior to meeting the seed pulse, these speckles can lead to significant divergence, self-focusing and filamentation of the pump beam [83]. In addition, the presence of speckles in the pump can lead to uneven amplification of the seed, since $\int a_0^2(t)dt$ is modulated across the spot area of the pump: the speckle pattern will be 'imprinted' on the amplified seed pulse. The use of beam smoothing techniques to smooth the probe pulse after amplification may be unfeasible due to the high intensities. Thus, reduction strategies of speckle effects need to be implemented before the pump and probe pulses interact. We anticipate the following ways to mitigate the effect of pump speckles. First, the use of wide spot areas for both pump and seed pulses, as we have considered in this work, can reduce the speckle-induced divergence of the pump beam.

Second, the pump beam can be smoothed using techniques such as random phase plates, induced spatial incoherence or smoothed spatial dispersion [84]. However, such techniques should be used with caution: in addition to smoothing the envelope of the pump beam, they will also reduce its capacity to drive stimulated Raman and Brillouin backscattering and amplification [26, 85, 86]. A third possible strategy to mitigate speckle effects could be to use spike trains of uneven duration and delay pulses [87, 88] for the pump beam: this enables the reduction of fluctuations in $\int a_0^2(t)dt$ across the spot of the pump beam and may therefore enable a more uniform amplification of the probe pulse. This is similar in spirit to previous work on Raman amplification using multiple pumps to reduce probe pulse precursors and generally improve the probe pulse envelope has been studied for Raman amplification by Balakin *et al* [89]. A similar approach can be used with Brillouin amplification. Further exploration of these non-ideal beam effects will be subject of future work.

5. Conclusions

We have identified a parameter regime where efficient ($\simeq 50\%$) amplification of laser pulses with high-quality (low levels of transverse filamentation) can be achieved via strong-coupling Brillouin scattering in over-quarter-critical density plasma. We have derived theoretical scalings for the competition between Brillouin amplification and seed pulse filamentation—the main limiting instability to obtaining high-quality Brillouin-amplified pulses at over-quarter-critical plasma densities. Our scalings indicate that the deleterious effects of seed pulse filamentation can be offset by operating at low pump intensities. Specifically, we show that for a fixed tolerance level of seed pulse filamentation, Brillouin compression and amplification ratios increase with decreasing pump intensity as $I_{\mathrm{pu}}^{-2/5}$.

Our theoretical scalings are supported by large-scale 2D (moving-window) PIC simulations that follow the evolution of the Brillouin-amplified seed pulse and its self-consistent interplay with ponderomotive filamentation. In particular, we obtained increasing amplification (compression) ratios of 15 (40), 30 (60), 40 (72) for decreasing pump intensities of 10^{16}, 10^{15} and 10^{14} W cm^{-2}, respectively, before transverse filamentation levels of the amplified seed exceeded 10%; the fluences of the amplified seed pulses were 6.5, 1.6 and 0.5 kJ cm^{-2}, respectively.

Together, our findings suggest that, for the right laser-plasma configurations, Brillouin amplification is a robust and reliable way to compress and amplify sub-picosecond laser pulses in plasma, and provide a comprehensive guide for the design and execution of future Brillouin amplification experiments. In a recent Brillouin amplification experiment by Marquès *et al* [19], Joule-level amplification was obtained when the parameters of the initial seed pulse obeyed our equation (2). However, the transverse spot of the amplified pulse still shows signs of filamentation in this experiment. Our work sheds light on how filamentation can be further controlled to improve the laser spot quality in similar experiments.

Data availability statement

The data that support the findings of this study are available upon reasonable request from the authors.

Acknowledgments

ORCID iDs

E P Alves ⬡ https://orcid.org/0000-0002-4588-1003
R M G M Trines ⬡ https://orcid.org/0000-0003-2553-0289
R Bingham ⬡ https://orcid.org/0000-0002-9843-7635
R A Cairns ⬡ https://orcid.org/0000-0002-7562-2053
R A Fonseca ⬡ https://orcid.org/0000-0001-6342-6226
L O Silva ⬡ https://orcid.org/0000-0003-2906-924X

References

[1] Maier M, Kaiser W and Giordmaine J A 1966 *Phys. Rev. Lett.* **17** 1275
[2] Milroy R D, Capjack C E and James C R 1977 *Plasma Phys.* **19** 989
[3] Milroy R D, Capjack C E and James C R 1979 *Phys. Fluids* **22** 1922
[4] Capjack C E, James C R and McMullin J N 1982 *J. Appl. Phys.* **53** 4046
[5] Andreev A A and Sutyagin A N 1989 *Sov. J. Quantum Electron.* **19** 1579
[6] Malkin V M, Shvets G and Fisch N J 1999 *Phys. Rev. Lett.* **82** 4448
[7] Kirkwood R *et al* 1999 *Phys. Rev. Lett.* **83** 2965
[8] Malkin V M, Shvets G and Fisch N J 2000 *Phys. Rev. Lett.* **84** 1208
[9] Ping Y *et al* 2004 *Phys. Rev. Lett.* **92** 175007
[10] Andreev A A *et al* 2006 *Phys. Plasmas* **13** 053110
[11] Ren J *et al* 2007 *Nat. Phys.* **3** 732–6
[12] Ping Y *et al* 2009 *Phys. Plasmas* **16** 123113
[13] Lancia L *et al* 2010 *Phys. Rev. Lett.* **104** 025001
[14] Trines R M G M *et al* 2011 *Nat. Phys.* **7** 87
[15] Kirkwood R K *et al* 2011 *Phys. Plasmas* **18** 056311
[16] Trines R M G M *et al* 2011 *Phys. Rev. Lett.* **107** 105002
[17] Toroker Z, Malkin V M and Fisch N J 2012 *Phys. Rev. Lett.* **109** 085003
[18] Lancia L *et al* 2016 *Phys. Rev. Lett.* **116** 075001
[19] Marquès J-R *et al* 2019 *Phys. Rev. X* **9** 021008
[20] Lehmann G, Spatschek K H and Sewell G 2013 *Phys. Rev. E* **87** 063107
[21] Lehmann G and Spatschek K-H 2013 *Phys. Plasmas* **20** 073112
[22] Lehmann G and Spatschek K H 2014 *Phys. Plasmas* **21** 053101
[23] Chiaramello M *et al* 2016 *Phys. Plasmas* **23** 072103
[24] Sadler J D *et al* 2017 *High Energy Density Phys.* **23** 212
[25] Sadler J D *et al* 2017 *Phys. Rev. E* **95** 053211
[26] Trines R M G M *et al* 2020 *Sci. Rep.* **10** 19875
[27] Sadler J D *et al* 2015 *Sci. Rep.* **5** 16755
[28] Edwards M R, Mikhailova J M and Fisch N J 2017 *Phys. Rev. E* **96** 023209
[29] Lehmann G and Spatschek K H 2015 *Phys. Plasmas* **22** 043105
[30] Chiaramello M, Amiranoff F, Riconda C and Weber S 2016 *Phys. Rev. Lett.* **117** 235003
[31] Vieira J *et al* 2016 *Nat. Commun.* **7** 10371
[32] Vieira J *et al* 2016 *Phys. Rev. Lett.* **117** 265001
[33] Edwards M R *et al* 2016 *Phys. Rev. Lett.* **116** 015004
[34] Kenan Q, Barth I and Fisch N J 2017 *Phys. Rev. Lett.* **118** 164801
[35] Schluck F, Lehmann G and Spatschek K H 2017 *Phys. Rev. E* **96** 053204
[36] Sadler J D *et al* 2018 *Commun. Phys.* **1** 19
[37] Edwards M R, Shi Y, Mikhailova J M and Fisch N J 2019 *Phys. Rev. Lett.* **123** 025001
[38] Kruer W L *et al* 1996 *Phys. Plasmas* **3** 382
[39] Williams E A *et al* 2004 *Phys. Plasmas* **11** 231
[40] Michel P *et al* 2009 *Phys. Plasmas* **16** 042702
[41] Glenzer S H *et al* 2010 *Science* **327** 1228
[42] Michel P *et al* 2010 *Phys. Plasmas* **17** 056305
[43] Hinkel D E *et al* 2011 *Phys. Plasmas* **18** 056312
[44] Moody J D *et al* 2012 *Nat. Phys.* **8** 344
[45] Tanaka K *et al* 1982 *Phys. Rev. Lett.* **48** 1179
[46] Walsh C J, Villeneuve D M and Baldis H A 1984 *Phys. Rev. Lett.* **53** 1445
[47] Villeneuve D M, Baldis H A and Bernard J E 1987 *Phys. Rev. Lett.* **59** 1585
[48] Baldis H A *et al* 1993 *Phys. Fluids B* **5** 3319
[49] Baton S D *et al* 1994 *Phys. Rev. E* **49** R3602
[50] Mori W B *et al* 1994 *Phys. Rev. Lett.* **72** 1482
[51] Langdon A B and Hinkel D E 2002 *Phys. Rev. Lett.* **89** 015003
[52] Lindl J D *et al* 2004 *Phys. Plasmas* **11** 339
[53] Hinkel D E *et al* 2005 *Phys. Plaasmas* **12** 056305
[54] Froula D H *et al* 2007 *Phys. Plasmas* **14** 055705
[55] Michel P *et al* 2011 *Phys. Rev. E* **83** 046409
[56] Glenzer S H *et al* 2011 *Phys. Rev. Lett.* **106** 085004
[57] Forslund D W *et al* 1985 *Phys. Rev. Lett.* **54** 558
[58] Decker C D, Mori W B and Katsouleas T 1994 *Phys. Rev. E* **50** R3338
[59] Rousseaux C *et al* 1995 *Phys. Rev. Lett.* **74** 4655
[60] Krushelnick K *et al* 1995 *Phys. Rev. Lett.* **75** 3681
[61] Tzeng K-C, Mori W B and Decker C D 1996 *Phys. Rev. Lett.* **76** 3332
[62] Decker C D *et al* 1996 *Phys. Plasmas* **3** 1360
[63] Moore C I *et al* 1997 *Phys. Rev. Lett.* **79** 3909
[64] Tzeng K-C and Mori W B 1998 *Phys. Rev. Lett.* **81** 104
[65] Gordon D *et al* 1998 *Phys. Rev. Lett.* **80** 2133
[66] Matsuoka T *et al* 2010 *Phys. Rev. Lett.* **105** 034801
[67] Forslund D W, Kindel J M and Lindman E L 1975 *Phys. Fluids* **18** 1002
[68] Max C E, Arons J and Langdon A B 1974 *Phys. Rev. Lett.* **33** 209
[69] Kim J, Lee H J, Suk H and Ko I S 2003 *Phys. Lett. A* **314** 464
[70] Weber S *et al* 2013 *Phys. Rev. Lett.* **111** 055004
[71] Riconda C *et al* 2013 *Phys. Plasmas* **20** 083115
[72] Fonseca R A *et al* 2002 *Lect. Notes Comput. Sci.* **2331** 342–51
[73] Fonseca R A *et al* 2003 *Phys. Plasmas* **10** 1979

[74] Fonseca R A *et al* 2008 *Plasma Phys. Control. Fusion* **50** 12

[75] Mardahl P *et al* 2001 *Bull. Am. Phys. Soc. 46, DPP 2001, KP1.108* (available at: https://ui.adsabs.harvard.edu/abs/2001APS..DPPKP1108M/abstract)

[76] Mardahl P 2001 PIC Code Charge Conservation, Numerical Heating, and Parallelization: Application of XOOPIC to Laser Amplification via Raman Backscatter *PhD Thesis* University of California, Berkeley

[77] Joshi C, Clayton C E and Chen F F 1982 *Phys. Rev. Lett.* **48** 874

[78] Sprangle P, Tang C-M and Esarey E 1987 *IEEE Trans. Plasma Sci.* **15** 145

[79] Shvets G and Pukhov A 1999 *Phys. Rev. E* **59** 1033

[80] Fraiman G M, Yampolsky N A, Malkin V M and Fisch N J 2002 *Phys. Plasmas* **9** 3617

[81] Hüller S, Mulser P and Rubenchik A M 1991 *Phys. Fluids* B **3** 3339

[82] Froula D H *et al* 2011 *Nat. Photon.* **12** 262

[83] Schmitt A J and Afeyan B B 1998 *Phys. Plasmas* **5** 503

[84] Lehmberg R H and Obenschain S P 1983 *Opt. Commun.* **46** 27

[85] Mostovych A N *et al* 1987 *Phys. Rev. Lett.* **59** 1193

[86] Obenschain S P *et al* 1989 *Phys. Rev. Lett.* **62** 768

[87] Hüller S and Afeyan B 2013 *EPJ Web Conf.* **59** 05009

[88] Hüller S and Afeyan B 2013 *EPJ Web Conf.* **59** 05010

[89] Balakin A A, Fraiman G M, Fisch N J and Malkin V M 2003 *Phys. Plasmas* **10** 4856